and the best fit is obtained when

$$\Sigma[t_k - t_0 - \eta(\alpha, s_k)/V_0]^2 = \text{minimum}\S \quad \text{(A2)}$$

Let δt_k represent the arbitrary deviation of a time measurement from the best-fit curve. The parameters describing the curve must change accordingly but in such a way that the sum of the squares of deviations from the curve is a minimum, i.e.,

$$\Sigma[t_k - t_0 - \delta t_0 - \delta\alpha(\partial\eta_k/\partial\alpha)/V_0 - \eta_k/V_0 - \eta_k\delta(1/V_0)]^2 = \min \quad \text{(A3)}$$

or

$$\Sigma[\delta t_\pi - t_{c_k} - \delta t_0 - \eta_k'\delta\alpha/V_0 - \eta_k\delta(1/V_0)]^2 = \min \quad \text{(A4)}$$

where t_{c_k} is the time given by the best-fit curve (Eq. A1) at station k. Taking the derivative of Eq. (A4) with respect to δt_0, $\delta\alpha$, and $\delta(1/V_0)$ and equating each to zero yields a set of three equations for δt_0, $\delta\alpha$, and $\delta(1/V_0)$ as a function of δt_k. Taking the derivative of each equation with respect to δt_k produces the following set of equations for $\partial t_0/\partial t_k$, $\partial\alpha/\partial t_k$, and $\partial(1/V_0)/\partial t_k$

$$\eta_k'/V_0 = (\partial\alpha/\partial t_k)\Sigma\eta_k'^2/V_0^2 + [\partial(1/V_0)/\partial t_k]\,\Sigma\eta_k\eta_k'/V_0 + (\partial t_0/\partial t_k)\Sigma\eta_k'/V_0$$

$$\eta_k = (\partial\alpha/\partial t_k)\,\Sigma\eta_k\eta_k'/V_0 + [\partial(1/V_0)/\partial t_k]\,\Sigma\eta_k^2 + (\partial t_0/\partial t_k)\,\Sigma\eta_k \quad \text{(A5)}$$

$$1 = (\partial\alpha/\partial t_k)\,\Sigma\,\eta_k'/V_0 + [\partial(1/V_0)/\partial t_k]\,\Sigma\eta_k + (\partial t_0/\partial t)_k N$$

Solving for $\partial\alpha/\partial t_k$, squaring and summing over k gives

$$\Sigma(\partial\alpha/\partial t_k)^2 = [N\Sigma\eta_k^2 - (\Sigma\eta_k)^2]V_0^2/D \quad \text{(A6)}$$

where

$$D = \begin{vmatrix} \Sigma\eta_k'^2 & \Sigma\eta_k'\eta_k & \Sigma\eta_k' \\ \Sigma\eta_k'\eta_k & \Sigma\eta_k^2 & \Sigma\eta_k \\ \Sigma\eta_k' & \Sigma\eta_k & N \end{vmatrix}$$

References

[1] Hodges, A. J., "The Drag Coefficient of Very High Velocity Spheres," *Journal of Aeronautical Sciences*, Vol. 24, No. 10, Oct. 1957, pp. 755–758.

[2] May, A. and Witt, W. R., "Free Flight Determination of the Drag Coefficients of Spheres," *Journal of Aeronautical Sciences*, Vol. 20, No. 9, Sept. 1953, pp. 635–638.

[3] Charters, A. C. and Thomas, R. N., "The Aerodynamic Performance of Small Spheres from Subsonic to High Supersonic Velocities," *Journal of Aeronautical Sciences*, Vol. 12, No. 4, Oct. 1945, pp. 468–476.

[4] Seiff, A., "A New Method for Computing Drag Coefficients from Ballistic Range Data," *Journal of Aeronautical Sciences*, Vol. 25, No. 2, Feb. 1958, pp. 133–134.

[5] Pitkin, E. T., "Determination of Flight Speeds and Drag Coefficients from Time and Distance Measurements," *Journal of Spacecraft and Rockets*, Vol. 5, No. 8, Aug. 1968, pp. 1000–1002.

[6] Bevington, P. R., *Data Reduction and Error Analysis for the Physical Sciences*, McGraw-Hill, New York, 1969, pp. 204–246.

[7] Baird, D. C., *Experimentation: An Introduction to Measurement Theory and Experiment Design*, Prentice Hall, Englewood Cliffs, N.J., 1968, p. 63.

[8] Crowe, C. T. et. al., "Measurement of Particle Drag Coefficients in Flow Regimes Encountered by Particles in a Rocket Nozzle," 2296-FR, Contract No. DAH-C04-67-C-0057, March 1969, United Technology Center, Sunnyvale, Calif.

[9] Slattery, J. C., Friichtenicht, J. F., and Hamermesh, B., "Interaction of Micrometeorites with Gaseous Targets," *AIAA Journal*, Vol. 2, No. 3, March 1964, pp. 543–548.

[10] Fraser, D. A. S., *Statistics, An Introduction*, Wiley, New York, 1958, p. 389.

§ All summations are performed from $k = 1$ to $k = N$.

A Comparison of Boundary-Layer Transition Data from Temperature-Sensitive Paint and Thermocouple Techniques

George G. Mateer*
NASA Ames Research Center, Moffett Field, Calif.

Nomenclature

M = Mach number
p = pressure
u = velocity
s = distance along model surface from nose
T = temperature
ρ = density
μ = viscosity

Subscripts

e = boundary-layer edge condition
t = total condition
∞ = freestream condition

References 1 and 2 demonstrated that the phase-change, temperature-sensitive paint technique is a reliable method for obtaining quantitative aerodynamic heating data. In Ref. 2, these data were used as an indicator of boundary-layer transition, and transition Reynolds numbers were compared with those from other investigations. However, an assessment of the method for quantitative measurements of transition could not be made from this comparison because of differences in transition data between facilities. Since the simplicity of the technique would make it particularly suited for transition studies on complex configurations, a study was made to determine whether the temperature-sensitive paint technique would yield the same quantitative results as more conventional methods.

Tests were conducted in the Ames Research Center's 3.5-ft hypersonic wind tunnel on 5° half-angle cones at a freestream Mach number of 7.4. The total temperature was nominally 1500°R and total pressures ranged from 200 to 1800 psia, accordingly, freestream unit Reynolds numbers varied from 0.9 to 8 × 10⁶/ft. Boundary-layer transition was determined from heat-transfer distributions obtained by the temperature-sensitive paint and from the thermocouple-calorimeter techniques. The thermocouple tests have been previously reported.[3] For the paint tests the model was 22.75 in. long and a paint was selected that changed phase (solid to liquid) at 200°F. Heating rates were deduced from photographs of the melt line as described in Ref. 1.

An example of heating-rate data is shown in Fig. 1. Paint and thermocouple data compare very well over the entire boundary layer (laminar, transitional, and turbulent). The

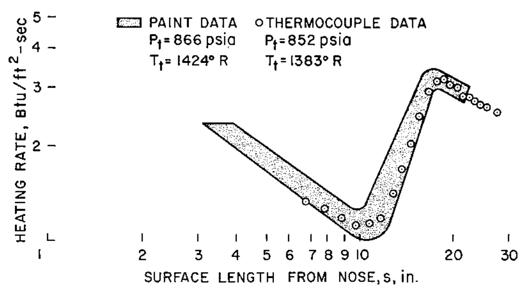

Fig. 1 Comparison of heating rates on 5° half-angle cones at $M_\infty = 7.4$.

Received August 13, 1970.

* Research Scientist. Associate Member AIAA.

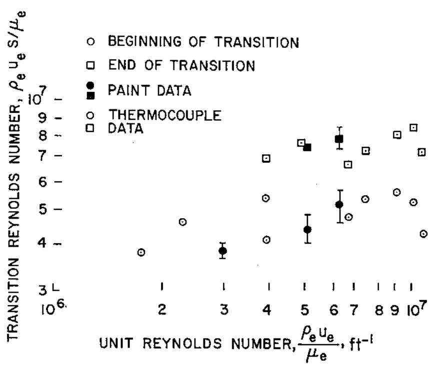

Fig. 2 Comparison of transition Reynolds numbers on 5° half-angle cones at $M_\infty = 7.4$.

location of the beginning and end of transition are also approximately the same. Similar paint data taken at other total pressures and transition Reynolds numbers are compared on Fig. 2.

The beginning of transition is defined as the intersection of straight lines faired through the laminar and transitional portions of the heating data. Similarly, the intersection of lines through the transitional and turbulent data defines the end of transition. Reynolds numbers based on surface distances to these intersections and boundary-layer-edge conditions are shown in Fig. 2 as a function of unit Reynolds number. Transition Reynolds numbers obtained using both paint and thermocouples compare very well and indicate that the paint technique can provide an adequate indication of boundary-layer transition.

References

[1] Jones, R. A. and Hunt, J. L., "Use of Fusible Temperature Indicators for Obtaining Quantitative Aerodynamic Heat-Transfer Data," TR-R-230, 1966, NASA.

[2] Stainback, P. C., "Some Effects of Roughness and Variable Entropy on Transition at a Mach Number of 8," *AIAA Journal*, Vol. 8, No. 1, Jan. 1970, pp. 173–175.

[3] Mateer, G. G. and Larson, H. K., "Unusual Boundary-Layer Transition Results on Cones in Hypersonic Flow," *AIAA Journal*, Vol. 7, No. 4, April 1969, pp. 660–664.

Optimum Relaxation Time for a Maxwell Core during Forced Vibration of a Rocket Assembly

Bernard W. Shaffer*
New York University, New York, N. Y.

AND

Robert I. Sann†
Ingersoll Rand Research Center, Princeton, N. J.

When the core of a case-bonded viscoelastic assembly is made of a Maxwell solid, an optimum relaxation time is found, which minimizes the displacement amplitude and the bond-stress response at resonance. For a Voigt solid the displacement amplitude and the bond-stress response at resonance decreases with retardation time, but no optimum time exists in the same sense.

In a previous paper concerned with the forced vibration response of a case-bonded viscoelastic cylinder,[1] the authors presented numerical results that indicated the existence of an optimum relaxation time τ for a Maxwell solid. At the optimum relaxation time τ the bond stress amplitude response is minimized. It was observed, on the basis of some numerical calculations, that the optimum relaxation time τ decreases with increasing values of the resonant frequency ω.

It is the purpose of this brief Note to prove the existence of an optimum relaxation time τ for an assembly consisting of a solid cylinder bonded to a thin casing, if the cylinder is made of a material which is a Maxwell solid. It is also demonstrated that a Voigt solid has no optimum retardation time.

The present analysis starts with the law of conservation of energy for the system. Neglecting thermodynamic effects, the law of conservation of energy may be written

$$P_{\text{ext}} = (d/dt)(KE) + \int_V \sigma_{ij}\dot{\epsilon}_{ij}dV \tag{1}$$

where σ_{ij} are the components of stress and $\dot{\epsilon}_{ij}$ are the components of strain rate; t is the parameter time. The term P_{ext} is the rate of work of the external forces, and KE is the kinetic energy of the system. The integral represents the rate of work done by the internal stresses during deformation.

There is no change in KE over one cycle of sinusoidal vibration. Hence, the integral of Eq. (1) from $t = 0$ to $t = 2\pi/\omega$ may be written

$$\int_0^{2\pi/\omega} P_{\text{ext}}dt = \int_0^{2\pi/\omega}\int_V \sigma_{ij}\dot{\epsilon}_{ij}dVdt \tag{2}$$

In the particular problem under consideration, which is the same as that previously studied,[1] the rate of work of the external force may be written

$$P_{\text{ext}} = \int_{-\pi}^{+\pi} -pa\frac{\partial}{\partial t}u(a,\theta,t)d\theta \tag{3}$$

where p is the normal surface traction applied to the outer surface of the casing, u is the radial displacement of particles under load, and a is the radius of the common surface between the cylinder and its casing.

It is convenient to separate the stress and strain-rate components into deviatoric components S_{ij}, e_{ij}, and its mean normal components σ,ϵ, respectively. If this is done, the product $\sigma_{ij}\dot{\epsilon}_{ij}$ can be written

$$\sigma_{ij}\dot{\epsilon}_{ij} = S_{ij}\dot{e}_{ij} + 3\sigma\dot{\epsilon} \tag{4}$$

Should be assumption again be made[1] that the cylinder is elastic in dilatation

$$\sigma = K\epsilon \tag{5}$$

where K is the bulk modulus of elasticity. The integral on the right side of Eq. (2) then becomes

$$\int_0^{2\pi/\omega}\int_V \sigma_{ij}\dot{\epsilon}_{ij}dVdt = \int_0^{2\pi/\omega}\int_V S_{ij}\dot{e}_{ij}dVdt \tag{6}$$

Equation (6) shows that all vibratory energy dissipation is due to distortion and none to volume change.

Let us write the pressure load $p(\theta,t)$ as a phasor

$$p = Re(P_0e^{j\omega t}) \tag{7}$$

where P_0 is the complex amplitude and ω the real frequency. Then the radial displacement $u(r,\theta,t)$ can be expressed

$$u = Re[(U_0/P_0)(j\omega,r)P_0e^{j\omega t}] \tag{8}$$

where the complex displacement transfer function $U_0(j\omega,r)/P_0$ is given explicitly by Eq. (37a) of Ref. 1; namely

$$\frac{U_0}{P_0} = \frac{aJ_1(\alpha r)}{[\rho a\omega^2 + 2G - hE/a(1-\nu^2)]J_1(z) - (K + \frac{4}{3}G)zJ_0(z)} \tag{9}$$

Received July 16, 1970. The results presented in this paper were obtained in the course of research sponsored by NASA under Grant No. NGR-33-016-067 to New York University. The authors wish to thank H. Yanowitz of the Perkin-Elmer Corporation for programing the example discussed in this report.

* Professor of Mechanical Engineering. Associate Fellow AIAA.

† Chief, Solid Mechanics Research. Member AIAA.